THE JOURNAL OF PHYSICAL CHEMISTRY A

Article

pubs.acs.org/JPCA

Numerical Implementation and Test of the Modified Variational Multiconfigurational Gaussian Method for High-Dimensional Quantum Dynamics

Miklos Ronto and Dmitrii V. Shalashilin*

School of Chemistry, University of Leeds, Leeds LS2 9JT, U.K.

ABSTRACT: In this paper, a new numerical implementation and a test of the modified variational multiconfigurational Gaussian (vMCG) equations are presented. In vMCG, the wave function is represented as a superposition of trajectory guided Gaussian coherent states, and the time derivatives of the wave function parameters are found from a system of linear equations, which in turn follows from the variational principle applied simultaneously to all wave function parameters. In the original formulation of vMCG, the corresponding matrix was not well-behaved and needed regularization, which required matrix inversion. The new implementation of the modified vMCG equations seems to have improved the method, which now enables straightforward solution of the linear system without matrix inversion, thus achieving greater efficiency, stability and robustness. Here the new version of the vMCG approach is tested against a number of benchmarks, which previously have been studied by split-operator, multiconfigurational time-dependent Hartree (MCTDH) and multilayer MCTDH (ML-MCTDH) techniques. The accuracy and efficiency of the new implementation of vMCG is directly compared with the method of coupled coherent states (CCS), another technique that uses trajectory guided grids. More generally we demonstrate that trajectory guided Gaussian based methods are capable of simulating quantum systems with tens or even hundreds of degrees of freedom previously accessible only for MCTDH and ML-MCTDH.

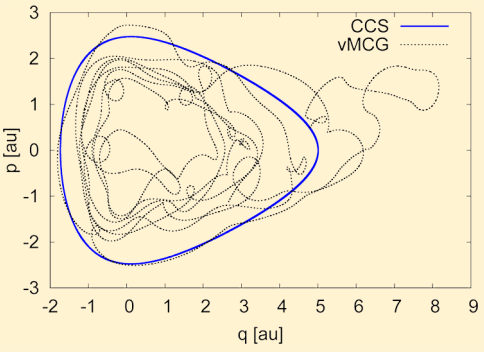

I. INTRODUCTION

Exact analytical solvability of the time-dependent Schrödinger equation for systems with large number of degrees of freedom (DOF) is limited to a few simple models. There are two problems that make multidimensional quantum mechanics difficult to deal with. First, determining the potential energy surface is a complicated problem, which is also present in classical molecular dynamics. Recently, substantial progress has been made[1,2] with various forms of PES parametrizations and fits. The second problem is the scaling of quantum mechanics with the number of degrees of freedom (DOF): the number of quantum states increases exponentially with the size of quantum system. Impressive progress has been made in calculations of quantum states for the systems comprised of large numbers of coupled vibrational modes[3] some of which can be very "floppy".[3,4] In dynamical calculations—when evolution of the wave packet is not restricted to a certain area—the "exponential curse" of quantum mechanics is perhaps the most severe. If a static grid of l states is used for a single-mode, a problem of M DOF requires

$$N = l^M \tag{1.1}$$

grid points, making the challenge of exponential scaling almost insurmountable.

In the past few decades a family of concepts based on trajectory guided Gaussians, which rely on locally defined adaptable basis sets, gained considerable importance. A number of methods both semiclassical and formally exact have been developed. The list of most important techniques can be divided into two categories. Semiclassical methods include but are not limited to the early application of frozen Gaussians[5] and semiclassical Herman−Kluk propagator.[6,7] For more details and new developments of the semiclassical Gaussian-based methods, see review.[8] Fully quantum techniques that at least in principle can be converged to a fully quantum result include multiple spawning,[9] Gaussian multiconfigurational time-dependent Hartree (G-MCTDH),[10] coupled coherent states (CCS),[11−13] variational Gaussian approach[14] and variational multiconfigurational Gaussians (vMCG).[15] All these techniques use grids (or basis sets) of trajectory-guided frozen Gaussian coherent states (CSs), which follow the wave function, thus economizing the basis set size. Another advantage of such techniques is that a randomly sampled basis can be used, which is advantageous in high-dimensional problems because Monte Carlo techniques scale with dimensionality much better than eq 1.1. Importance sampling, which is the crucial part of all the above methods, allows the basis to be built only around the dynamically important phase-space region. With such random

Special Issue: Joel M. Bowman Festschrift

Received: November 6, 2012
Revised: April 8, 2013
Published: April 15, 2013

   dx.doi.org/10.1021/jp310976d | J. Phys. Chem. A 2013, 117, 6948−6959

sampling, the Gaussian based methods can potentially scale quadratically as $N \propto M^2$, although in reality the scaling is often worse than that. However, even with the ever increasing computational power, the methods based on trajectory-guided Gaussians sometimes suffer from two difficulties: scaling and robustness.

VMCG[10,15] is potentially one of the most efficient CS-based methods of high-dimensional quantum dynamics. In vMCG, the wave function is represented as a superposition of N trajectory-guided Gaussian wave packets

$$|\Psi(t)\rangle = \sum_{n=1,N} a_n(t)|\mathbf{p}_n(t), \mathbf{q}_n(t)\rangle = \sum_{n=1,N} a_n(t)|\mathbf{z}_n(t)\rangle \tag{1.2}$$

The time evolution of the wave function can be determined from the variational principle. It yields time derivatives of its parameters, which can be obtained from a system of linear equations

$$\mathbf{D}\dot{\boldsymbol{\alpha}} = \mathbf{b} \tag{1.3}$$

where $\boldsymbol{\alpha}$ is the vector of wave function parameters, which includes both the amplitudes a_n and all positions $\mathbf{z}_n$ of N CSs (each one of them M-dimensional $\mathbf{z}_n = z_n^{(1)}, ..., z_n^{(M)}$) and $\mathbf{D}$ is the matrix that can be derived, for example, using the elegant formalism developed by Kramer and Saraceno[16] (See ref 17 for more details). Matrix $\mathbf{D}$ in eq 1.3, as well as similar matrices in other variational approaches,[18−21] is often numerically nearly singular and has to be regularized. This may be done by matrix inversion, during which the lowest eigenvalues of $\mathbf{D}$ are increased by a small and somewhat arbitrary regularization parameter so that the inverse matrix does not have extremely large elements. As a result, the equation is eventually written as

$$\dot{\boldsymbol{\alpha}} = \mathbf{D}^{-1}\mathbf{b} \tag{1.4}$$

which is of course equivalent to eq 1.3 from the formal point of view. Numerically, however, matrix inversion is much more expensive than the solution of system of linear eqs 1.3.

In a recent paper,[17] the equations of vMCG were modified and written in a form similar to the equations of the CCS technique,[12] another method based on trajectory guided Gaussians. In CCS, special efforts were made to minimize coupling between the amplitudes by making the coupling matrix small, smooth and sparse. CCS introduces a preexponential factor to smooth out the rapid oscillations of quantum amplitudes. It appears that this simple trick works also for vMCG and makes matrix $\mathbf{D}$ sufficiently well behaved. In the tests of the vMCG equations[17] presented here, we were able to solve eq 1.3 without inverting the matrix. Since our version of vMCG is closely connected to the CCS theory, we also compare the accuracy and efficiency of the two techniques. With the same basis size, vMCG is more accurate simply because it employs more variational parameters, as the time dependence of all the parameters in eq 1.2 are determined variationally. For the same number of variational parameters, however, the accuracy of the two techniques is close, and both methods show similar levels of robustness and stability.

In section II we briefly sketch our version of the vMCG theory, which, in the original paper,[17] was presented for the one-dimensional (1D) case only. Here we present the theory in multidimensional form, which is conceptually simple but involves long algebra, given in the Appendix A1. Chapter III provides details of the numerical tests. First, our implementation of vMCG was tested on simple Morse oscillator because a 1D problem allows one to visualize complicated variational trajectories. Then Henon−Heiles (HH) model was investigated, and the accuracy and efficiency of vMCG was compared with those of CCS, using the MCTDH benchmark obtained previously for 2D, 6D, 10D and 18D HH systems.[22] To demonstrate the limitations of vMCG and its scaling with the number of degrees of freedom, we also performed CCS calculation for 1458D model previously studied in ref 23 by ML-MCTDH, and show that vMCG calculation for a system of such size is not feasible, but CCS yields a good result. We also use this example to make some general remarks about the accuracy and convergence of vMCG, CCS, MCTDH and ML-MCTDH methods[24] of high-dimensional quantum mechanics.

Throughout this paper, natural units were used with $\hbar = 1$, and the CSs were set to have $\omega = 1$ and $m = 1$.

II. THEORY

II.1. Coherent States. In recent years, CS-based approaches gained considerable importance in molecular dynamics. As they are minimum uncertainty states and Gaussian-functions, they are compatible with both semiclassical and quantum mechanical descriptions. A single-mode CS z is an element of the phase-space $\Gamma = \{(q,p)\}$, where q_i and p_i are canonically conjugated variables. Using phase space coordinates, a 1D CS $z \in \mathbb{C}$ can be written as

$$z = \sqrt{\frac{\gamma}{2}}\, q + \frac{i}{\hbar}\sqrt{\frac{1}{2\gamma}}\, p \tag{2.1}$$

and

$$z^* = \sqrt{\frac{\gamma}{2}}\, q - \frac{i}{\hbar}\sqrt{\frac{1}{2\gamma}}\, p \tag{2.2}$$

with $\gamma = m\omega/\hbar$, where z and z^* are eigenstates of the annihilation and creation operators:

$$\hat{a}|z\rangle = z|z\rangle \tag{2.3}$$

$$\langle z|\hat{a}^\dagger = \langle z|z^* \tag{2.4}$$

A multidimensional CS is a product of m single-mode CSs:

$$|\mathbf{z}_i(t)\rangle = \prod_{k=1}^{m} |z_i^{(k)}(t)\rangle \tag{2.5}$$

and represents a point in M-dimensional phase space $\Gamma_M = \{(q_m,p_m);\ m = 1,2,...,M\}$. The overlap of two M-dimensional CSs

$$\begin{aligned}\boldsymbol{\Omega}_{ij} &= \langle \mathbf{z}_i|\mathbf{z}_j\rangle \\ &= \exp\left(\mathbf{z}_i^*\mathbf{z}_j - \frac{\mathbf{z}_i\mathbf{z}_i^*}{2} - \frac{\mathbf{z}_j\mathbf{z}_j^*}{2}\right) \\ &= \prod_{k=1}^{M} \langle z_i^{(k)}|z_j^{(k)}\rangle \\ &= \prod_{k=1}^{M} \exp\left(z_i^{*(k)}z_j^{(k)} - \frac{|z_i^{(k)}|^2}{2} - \frac{|z_j^{(k)}|^2}{2}\right)\end{aligned} \tag{2.6}$$

is a product of M 1D overlaps. Although continuum basis of CSs is overcomplete in numerical calculations, we always deal with a finite set of CSs that simply represent a nonorthogonal

dx.doi.org/10.1021/jp310976d | J. Phys. Chem. A 2013, 117, 6948−6959

basis with the overlap matrix 2.6. In this finite basis of CS the identity becomes

$$\mathbb{I} = \sum_{ij} |\mathbf{z}_i\rangle \mathbf{\Omega}_{ij}^{-1} \langle \mathbf{z}_j| \tag{2.7}$$

where $\mathbf{\Omega}_{ij}^{-1}$ are the elements of the inverse overlap matrix of CS. The identity 2.7 is a discretization of that of the continuous manifold covering all z-space where $\mathbb{I}$ is the product of M 1D integral identities

$$\mathbb{I} = \prod_{k=1}^{M} \left(\frac{1}{\pi} \int |z^{(k)}\rangle \langle z^{(k)}| \mathrm{d}^2 z^{(k)} \right) \tag{2.8}$$

with the single-mode integral measure $\mathrm{d}^2 z = (\mathrm{d}q\ \mathrm{d}p)/2\hbar$. For more details about CS notations, refer to ref 12. With the CS representation, any time-dependent wave function and its conjugate can be written up in CS basis in the general form 1.2. In coordinate representation, a CS is simply a multidimensional Gaussian wave packet with the following ansatz:

$$\langle \mathbf{x}_i | \mathbf{z}_j \rangle = \left(\frac{\gamma}{\pi} \right)^{m/4} \exp\left(-\frac{\gamma}{2} (\mathbf{x}_i - \mathbf{q}_i)^T (\mathbf{x}_i - \mathbf{q}_i) + \frac{i}{\hbar} \mathbf{p}_j (\mathbf{x}_i - \mathbf{q}_i) + \frac{i \mathbf{p}_j \mathbf{q}_j}{2\hbar} \right) \tag{2.9}$$

Matrix elements of an arbitrary operator can be found via its normal ordered form $:O(\hat{a}^\dagger, \hat{a}):$ in which the powers of the creation operator precede those of the annihilation operator if $\hat{a}^\dagger$,$\hat{a}$ are replaced by corresponding z or its complex conjugate and the result is multiplied by the overlap:

$$\langle z | :O(\hat{a}^\dagger, \hat{a}): | z' \rangle = \langle z | z' \rangle O_{\mathrm{ord}}(z^*, z) \tag{2.10}$$

This is also applicable to the single-mode Hamilton operators:

$$\langle z | :H(\hat{a}^\dagger, \hat{a}): | z' \rangle = \langle z | z' \rangle H_{\mathrm{ord}}(z^*, z) \tag{2.11}$$

The index "ord" simply reminds about the terms that originated from commuting $\hat{a}^\dagger$,$\hat{a}$. The Hamilton operator of the system is the sum over the dimensions of the individual single-mode Hamiltonians and their coupling terms:

$$\langle \mathbf{z}_i | :\mathbf{H}(\hat{a}^{\dagger(k)}, \hat{a}^{(k)}): | \mathbf{z}_j \rangle = \mathbf{\Omega}_{ij} \mathbf{H}_{\mathrm{ord}}(\mathbf{z}_i^*, \mathbf{z}_j) \tag{2.12}$$

2.2. Dynamics. Time-dependent variational principle (TDVP) provides a generic way to derive various forms of the time-dependent Schrödinger equation. Several formulations of TDVP exist;[16,18−21] our description here is based on the approach[16] where TDVP is presented in a form similar to the principle of least action in classical mechanics and defining equations of motion through Euler−Lagrange equations. According to the principle of least action, the equations of motion can be obtained from the extremum of the functional

$$\sigma = \int_{t_2}^{t_1} \Lambda(\boldsymbol{\alpha}, \boldsymbol{\alpha}^*, \dot{\boldsymbol{\alpha}}, \dot{\boldsymbol{\alpha}}^*)\, \mathrm{d}t \tag{2.13}$$

where the Lagrangian is

$$\Lambda = \langle \Psi(t) | i \overrightarrow{\partial}_t - H | \Psi(t) \rangle \tag{2.14}$$

with the differential-operator $\overrightarrow{\partial}_t$ acting separately on bras and kets. Any state vector $|\Psi\rangle$ can be rewritten in CS form 1.2 $|\Psi(\boldsymbol{\alpha}(\mathrm{t}))\rangle = |\Psi(a(\mathrm{t}),\mathbf{z}(\mathrm{t}))\rangle$, and therefore the Lagrangian can be reparametrized with amplitudes and CS phase space positions as[17]

$$\begin{aligned} \Lambda(\boldsymbol{\alpha}, \boldsymbol{\alpha}^*, \dot{\boldsymbol{\alpha}}, \dot{\boldsymbol{\alpha}}^*) &= \Lambda(a, \mathbf{z}, a^*, \mathbf{z}^*, \dot{a}, \dot{\mathbf{z}}, \dot{a}^*, \dot{\mathbf{z}}^*) \\ &= \frac{i}{2} \sum_{ij} \mathbf{\Omega}_{ij} \Big[a_i^* \dot{a}_j - \dot{a}_i^* a_j + a_i^* a_j \Big(\mathbf{z}_i^* \dot{\mathbf{z}}_j - \dot{\mathbf{z}}_i^* \mathbf{z}_j \\ &\quad - \frac{1}{2} (\mathbf{z}_j^* \dot{\mathbf{z}}_j + \dot{\mathbf{z}}_j^* \mathbf{z}_j - \mathbf{z}_i^* \dot{\mathbf{z}}_i - \dot{\mathbf{z}}_i^* \mathbf{z}_i) + 2i \mathbf{H}_{\mathrm{ord}}(\mathbf{z}_i^*, \mathbf{z}_j) \Big) \Big] \end{aligned} \tag{2.15}$$

where $\boldsymbol{\alpha} = \{a,\mathbf{z}\}$ is the vector of the wave function parameters that includes all $N \times M$ components of the M-dimensional complex vectors $\mathbf{z}_{j=1,N}$ describing the phase space positions of all basis CSs and N their amplitudes $a_{j=1,N}$. Quantum equations of motion can now be written as standard Lagrange equations for the wave function parameters

$$\frac{\partial \Lambda}{\partial \boldsymbol{\alpha}} - \frac{\mathrm{d}}{\mathrm{d}t} \frac{\partial \Lambda}{\partial \dot{\boldsymbol{\alpha}}} = 0 \tag{2.16}$$

which, after introduction of a conjugated momentum $\pi_\alpha = 2\frac{\partial \Lambda}{\partial \dot{\alpha}}$ can be presented in the form of Hamilton's equations[16]

$$\mathbf{D} \dot{\boldsymbol{\alpha}} = \frac{\partial \langle \mathcal{H} \rangle}{\partial \boldsymbol{\alpha}^*} \tag{2.17}$$

where $\mathbf{D}$ is the matrix with the elements $D_{ij} = \partial \pi_{\alpha_i} / \partial \alpha_j^*$ and $\langle \mathcal{H} \rangle$ is the effective Hamiltonian obtained from the Lagrangian (eq 2.14) in the usual way as $\langle \mathcal{H} \rangle = \boldsymbol{\pi}_\alpha \boldsymbol{\alpha} - \Lambda$. The operator $\langle \mathcal{H} \rangle$ should not be confused with the actual physical Hamiltonian of the system. The Lagrangian Λ and the effective Hamiltonian $\langle \mathcal{H} \rangle$ are simply a tool to formally work out the quantum equations of motion. We have used Greek letters π, σ, and Λ to denote general momentum, action and the Lagrangian associated with it to distinguish them from p, S and L, the momentum, action and Lagrangian of the actual trajectory of a physical coordinate q. More details about the equations and their derivation can be found in ref 17 and in Appendix A1. Here we only point out that equations[17] have been written not for the oscillating amplitude

$$a_j = d_j \exp(iS_j) \tag{2.18}$$

but for smooth preexponential factor d_j, where S_j is the action along the trajectory. As a result, matrix $\mathbf{D}$ in eq 2.17 has many small elements and is therefore sparse and smooth.

In vMCG, at each time step, one has to find the derivatives of the parameters from the system of coupled $N \times (M + 1)$ linear eqs 2.17, where N is the basis set size and M is the number of degrees of freedom. CCS is another method that utilizes exactly the same parametrization of the wave function 1.2 as vMCG. The difference is that in CCS the trajectories $\mathbf{z}_n(t)$ are predetermined and calculated from essentially classical equations of motion. Only N amplitudes $d_n(t)$ are found from quantum variational principle. As a result, the system of linear equations for the derivatives of $d_n(t)$ is much smaller and much simpler than in vMCG. Matrix $\mathbf{D}$ used in vMCG has the size of $[N \times (M + 1)] \times [N \times (M + 1)]$ and includes that of CCS as a small $N \times N$ block. The elements of this small $N \times N$ matrix are simply those of the overlap matrix multiplied by the exponentials of the classical actions. CCS trajectories are driven by a classical Hamiltonian with quantum corrections $\mathbf{H}_{\mathrm{ord}}$ (eq 2.12), which is simply the expectation value of the classical Hamiltonian with the Gaussian CS. The mathematical structure of the two methods has been compared in ref 17. In this paper,

dx.doi.org/10.1021/jp310976d | J. Phys. Chem. A 2013, 117, 6948−6959

we compare their computational cost and accuracy. At first glance, vMCG appears more expensive than CCS. However, as it will be shown below, as vMCG works with a smaller basis than CSs, the computational cost of the two related methods is comparable.

III. NUMERICAL IMPLEMENTATION AND RESULTS

3.1. Basis Set Sampling. First we have tested vMCG in the form given in ref 17 on the examples of 1D harmonic and 1D Morse oscillators. Then we employed the multidimensional HH model in 2D, 6D, 10D, 18D and 1458D. The results were compared with CCS and with the benchmarks provided earlier by MCTDH[22] and ML-MCTDH.[23] Since both CCS and vMCG utilize the grids of trajectory guided CSs we also compare their accuracy and efficiency. In both CCS and vMCG methods, the initial propagating wave function is itself a CS $\mathbf{z}_0$:

$$|\Psi(0)\rangle = |\mathbf{z}_o\rangle \tag{3.1}$$

In both approaches, the sampling of the Gaussian CS basis is very important, and we have used the same techniques suggested previously in ref 11 to select initial conditions for the basis set $|\mathbf{z}_j\rangle$. The simplest way to bias the basis to the dynamically important region would be to use the "compressed swarm". The initial phase space positions of CSs $|\mathbf{z}_j\rangle$ have been chosen randomly from a Gaussian distribution centered around $\mathbf{z}_o$

$$f(\mathbf{z}_j) = \frac{1}{\pi^m} \exp(-\delta\,|\mathbf{z}_j - \mathbf{z}_o|^2) \tag{3.2}$$

Then the initial amplitudes of $|\mathbf{z}_j\rangle$ are calculated by applying the identity 2.7 as follows

$$|\Psi(0)\rangle = \sum_j a_j(0)|\mathbf{z}_j(0)\rangle = \sum_{ij} |\mathbf{z}_j(0)\rangle \mathbf{\Omega}^{-1}_{ji}\mathbf{z}_i(0)|\Psi(0)\rangle \tag{3.3}$$

In eq 3.2 the "compression" parameter δ determines the degree of bias of the basis set to its center $\mathbf{z}_o$. The smaller is the basis set, the more compressed the distribution should be. Parameter δ is chosen such that the norm of the wave function

$$\langle\Psi(0)|\Psi(0)\rangle = \sum_{ij} \langle\Psi(0)|z_j(0)\rangle \mathbf{\Omega}^{-1}_{ji}\langle z_i(0)|\Psi(0)\rangle \approx 1 \tag{3.4}$$

is close to 1, which is not the case for a small basis that is not "compressed" well enough. The norm $\langle\Psi|\Psi\rangle$ was always kept in the range between 0.990 and 0.995. With the sampling discussed above, the two methods (CCS and vMCG) can be compared on equal footing. The sampling described above is called Sampling 1 (S1) and used for the majority of the tests.

We also tried another sampling called S2, where the propagating CS $|\Psi(0)\rangle = |\mathbf{z}_o\rangle$ was included in the basis, such that the first basis function is

$$|\mathbf{z}_{j=1}\rangle = |\mathbf{z}_o\rangle \tag{3.5}$$

The rest of the basis was chosen randomly as in the sampling S1. In sampling S2, the initial conditions for the amplitudes are $d_j = 1$ if $j = 1$ and $d_j = 0$ if $j \neq 1$. These conditions are further described in Appendix A2.

Another type of sampling strategy (S3) was used for the 1458D HH model where only two modes are excited initially, and the rest of the modes act like a "bath". For a multidimensional initial wave function $|\Psi^{(k)}(0)\rangle$, for every mode k, a different compression parameter $\delta^{(k)}$ can be chosen, therefore different compression can be applied for the excited "system" modes and for the "bath" modes. This allows one to treat more important modes with less compression and therefore with less bias. This sampling strategy is called "pancake" distribution and has successfully been used for CCS previously.[11,25] In the 1458D HH system investigated, two adjacent modes (exc_1 and exc_2) are excited in the middle of the chain, for these modes no compression was applied in the sampling (i.e., $\delta^{(\text{exc1})} = \delta^{(\text{exc2})} = 1$). For the "bath" modes, the compression was applied according to the function

$$\delta^{(k)} = \exp\left(\frac{k - \frac{\text{exc}_1 + \text{exc}_2}{2}}{\Delta}\right)^2 \tag{3.6}$$

where parameter Δ gives the width of the discrete Gaussian distribution. Geometrically, this means that the compression rapidly increases for the sampling of less important "bath" modes, which are far from the excited modes exc_1 and exc_2.

3.2. Harmonic Oscillator and 1D Morse Oscillator. For the harmonic oscillator, both CCS and vMCG give exact solution, and their amplitudes and trajectories are identical. This is due to the fact that with the Hamiltonian of the harmonic oscillator, vMCG equations are equivalent to CCS equations. The simple 1D Hamiltonian of a Morse oscillator

$$H = \frac{p^2}{2} + D_e(\exp(-2\beta x) - 2\exp(-\beta x)) \tag{3.7}$$

with the energy parameter $D_e = 10.25$ *au*, the parameter $\beta = 0.2209$, and initial condition at $|\Psi(0)\rangle = |\mathbf{z}_0\rangle = |q = 5, p = 0\rangle$, has also been investigated. This system has been previously used to test CCS[26,27] and other related techniques. Methods such as vMCG and CCS are suited for high-dimensional problems, and for a 1D problem, CS-based methods do not have advantages before standard techniques. Moreover, if the CS basis becomes too large (which, for 1D or 2D problems, is often just a few tens of CSs) the overlap matrix in CCS and matrix $\mathbf{D}$ of vMCG become singular making propagation numerically unstable. This challenge justifies using simple 1D Harmonic and Morse oscillator models as a test problem. Also, a 1D problem allows one to visualize complicated vMCG trajectories. Figure 1 shows the autocorrelation function obtained by the vMCG method and compares it with that of numerically exact split-operator propagation. Figure 2 shows the guiding trajectories from vMCG methods, which are very

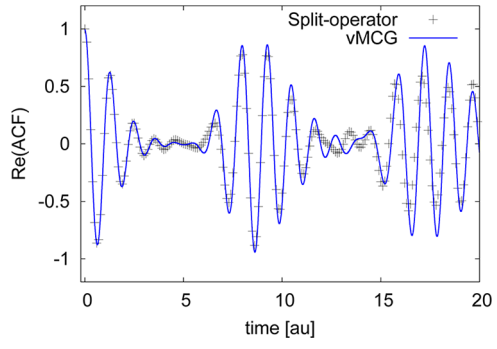

Figure 1. Real part of the autocorrelation function of a 1D Morse potential given by vMCG with the basis set size of 10 CSs (solid line), compared to results from the split-operator method (crosses).

dx.doi.org/10.1021/jp310976d | J. Phys. Chem. A 2013, 117, 6948−6959

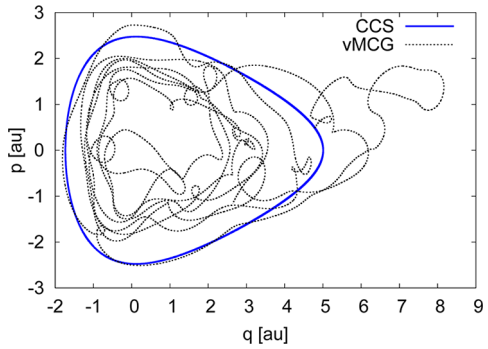

Figure 2. Typical complicated quantum variational trajectories of a 1D Morse potential with vMCG (dashed line) and simple CCS (solid line).

different from those of classical mechanics and almost classical CCS trajectories. The quantum vMCG trajectories are "pushed" by each other and by their amplitudes.

We found that for the sampling S1, the equations of vMCG[17] produce an accurate autocorrelation function without matrix inversion and regularization. For sampling S2, when propagation of the CS $|z_0\rangle$ is included into the basis and all initial amplitudes except one are zero, the vMCG system of linear equations is not well-defined, and the propagation is numerically unstable. Inspection of the matrix **D** reveals the presence of rows and columns with all elements equal to zero (Appendix A2), which makes its determinant zero. This has also been noted for the standard implementation of vMCG.[15] Propagation with the CCS method is stable for both sampling S1 and S2. For the S1 sampling, vMCG propagation for 1D harmonic and Morse oscillators worked with the same time step as CCS, and therefore the new version of vMCG was as robust and as stable as CCS. In the case of sampling S2, vMCG can be made free of numerical instabilities by either regularizing the matrix at the first step as it has been done in ref 15, or by propagating the system with CCS for a few steps and switching back to vMCG as soon as all amplitudes become nonzero.

3.3. HH Model. Multidimensional HH potential with strong coupling between the modes provides a more challenging benchmark for vMCG and other methods of high-dimensional quantum mechanics. The potential

$$V(q) = \frac{1}{2}\sum_{k=1}^{m} q_k^2 + \lambda \sum_{k=1}^{m-1}\left(q_k^2 q_{k+1} + \frac{1}{3}q_{k+1}^3\right) \tag{3.8}$$

is multidimensional, anharmonic, unbound and includes coupling terms between the modes with the coupling constant $\lambda = 0.111803$. The vMCG calculations were compared with CCS for 2D, 6D, 10D and 18D HH systems. In the 2D case, comparison can be made with the split-operator method, while 6D and 10D results can be compared with the benchmark MCTDH[22] and CCS calculations. In the case of the 18D model, the ML-MCTDH benchmark is available[23] for the standard HH model and the "strong coupling" model with coupling constant twice that of the standard parameter $\lambda = 2 \times 0.111803$. In addition, ref 23 reported a calculation for a 1458D HH model. The HH model was also previously used to test semiclassical Gaussian based techniques.[28,29]

For 2D, 6D and 10D models, the initial conditions were the same for both CCS and vMCG: the initial state is placed at $|\Psi(0)\rangle = |\mathbf{z}_0\rangle = |q = 2, p = 0\rangle \ldots |q = 2, p = 0\rangle$ (i.e., initially all modes are stretched and have zero momentum). Those basis CSs that become so energetic that they escape to the distance $q > 10$ were automatically removed from the calculations. Figures 3−8 show the real part of the autocorrelation function (ACF) for 2D, 6D and 10D HH potential.

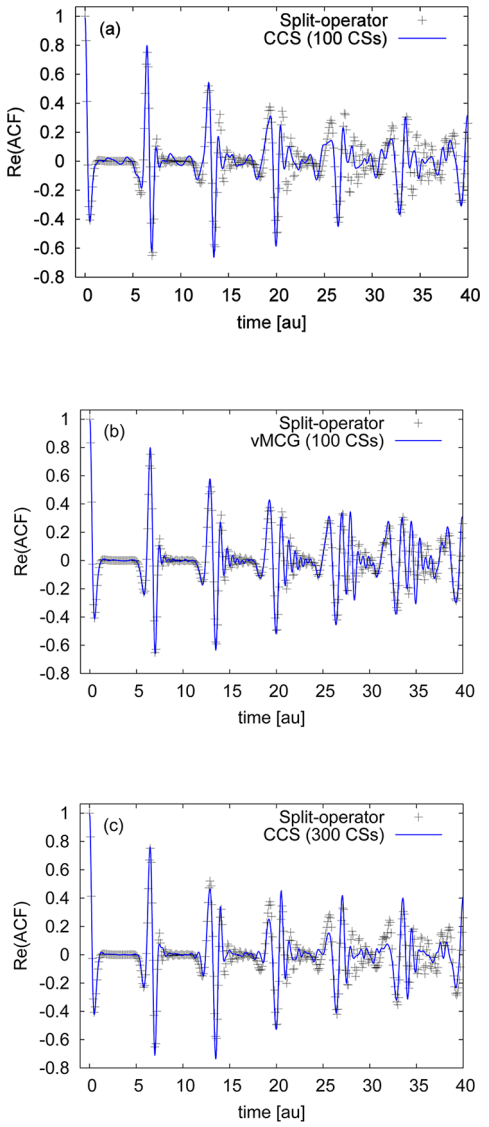

Figure 3. Real part of the autocorrelation function for the 2D HH problem. CCS and vMCG with the basis of 100 CSs (frames a and b). CCS with the basis of 300 CSs and therefore with the same number of variational parameters (frame c). The results are compared with those of the split-operator method (crosses).

For the 2D model, the time step of vMCG propagation was reduced to $\Delta t = 0.01$ to be able to run it stably, while CCS was still robust with $\Delta t = 0.1$ in all the cases. Therefore, vMCG can be less stable for lower dimensional systems (1D or 2D) but reducing time step solves the problem and it still works well. For the basis set size used (i.e., 100), the result of vMCG is visibly better than that of CCS. However CCS improves if the basis is increased to 300 CSs such that the number of variational parameters for both methods is the same. The time step used for the latter case was $\Delta t = 0.01$, but it also worked with longer time step.

For both vMCG and CCS we observed similar behavior in 6D and 10D cases shown in Figures 4−8. Running time was

dx.doi.org/10.1021/jp310976d | J. Phys. Chem. A 2013, 117, 6948−6959

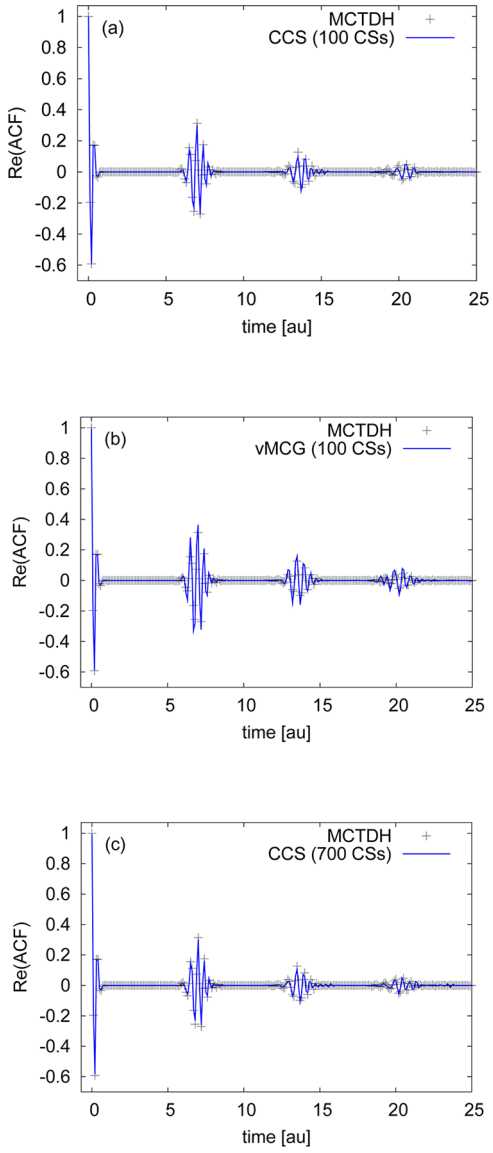

Figure 4. Real part of the autocorrelation function for the 6D HH problem. CCS and vMCG with the basis of 100 CSs (frames a and b). CCS with the basis of 700 CSs and therefore with the same number of variational parameters (lower frame c). The results are compared with those of the MCTDH method (crosses).

t_{max} = 20 with time step of Δt = 0.1 for both cases of CCS and vMCG. The initial norm was kept close to $\langle\Psi|\Psi\rangle$ = 0.9905 by setting the compression parameter. For the 10D case, we compared the deviation of vMCG and CCS from the MCTDH result. To quantify the quality of propagation for the 10D case, the deviation from benchmark MCTHD was calculated for the first (Figures 6 and 7) and the second recurrence (Figure 8) for both CCS and vMCG. The comparison of the results can be seen in Tables 1 and 2, respectively. Deviation is defined as the integral of the modulus of the difference between the real parts of the two autocorrelation functions. The conclusion is that, for the same number of variational parameters, both CCS and vMCG perform on the same level of accuracy. In high-dimensional 6D and 10D cases, the time step was the same for both vMCG and CCS, and vMCG performance was sufficiently robust and stable.

Two different 18D HH systems were investigated, and the results are shown in Figures 9−11, which present the absolute value of the autocorrelation function. The first system had the coupling constant λ = 0.111803 as in the previous cases of 2D, 6D and 10D models, and the second system had a stronger coupling λ = 0.223606 increased by the factor of 2. Only the modes 4, 8, 12 and 16 were excited $|\Psi^{(4)}(0)\rangle = |\Psi^{(8)}(0)\rangle = |\Psi^{(12)}(0)\rangle = |\Psi^{(16)}(0)\rangle = |q = 2, p = 0\rangle$ in both the standard and stronger coupling cases. For 18D HH simulations, the running time was t_{max} = 60, and the time step had to be reduced to Δt = 0.05 for CCS and Δt = 0.01 for vMCG. The initial norm was set with the compression parameter to be close to $\langle\Psi|\Psi\rangle$ = 0.993. The results of the standard and strong coupling can be seen in Figures 9−11. These results were compared with ML-MCTDH simulations[23] (Figure 9a) and (Figure 10a). For CCS, 3000 basis vectors were used, while in the case of vMCG the basis set size was 150 CSs; however, essentially the same result can be obtained with 1000 CSs for CCS and 50 CSs for vMCG (frame b in Figures 9−10) so that both vMCG and CCS calculations were well converged. The strongly coupled HH model is a more demanding problem: after a few oscillations, the autocorrelation function decays so rapidly that it almost vanishes. In Figure 11, the CCS and vMCG results are shown, compared with ML-MCTDH results. Although a relatively large basis set was used (4000 CSs for CCS and 200 for vMCG), the running time of the simulation was shorter compared to the previous case of standard HH model. This is due to the trajectories of the basis CSs escaping from the well of the HH potential and being removed from the propagation. By the end of the propagation, only 300 CSs were left in the case of CCS and only 8 for vMCG, making the basis very small. The quality of basis can be easily improved by generating new basis functions instead of escaping ones, but we have not done it in

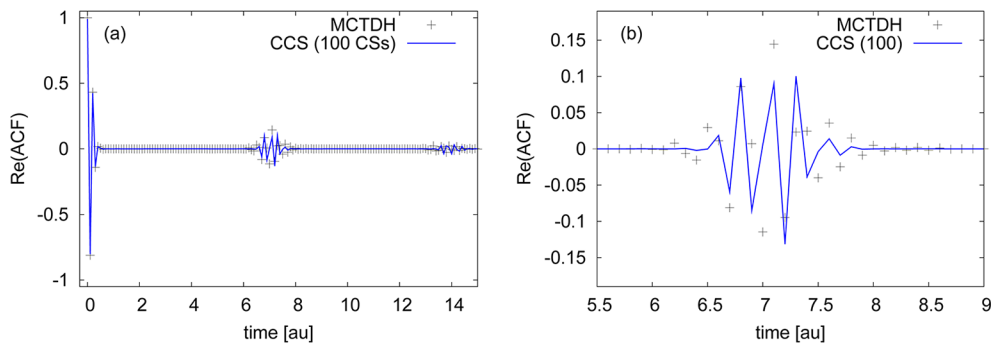

Figure 5. Real part of the autocorrelation function for the 10D HH problem with CCS with the basis of 100 CSs (solid line) compared with results from MCTDH (crosses) (frame a) and the first recurrence (frame b).

dx.doi.org/10.1021/jp310976d | J. Phys. Chem. A 2013, 117, 6948−6959

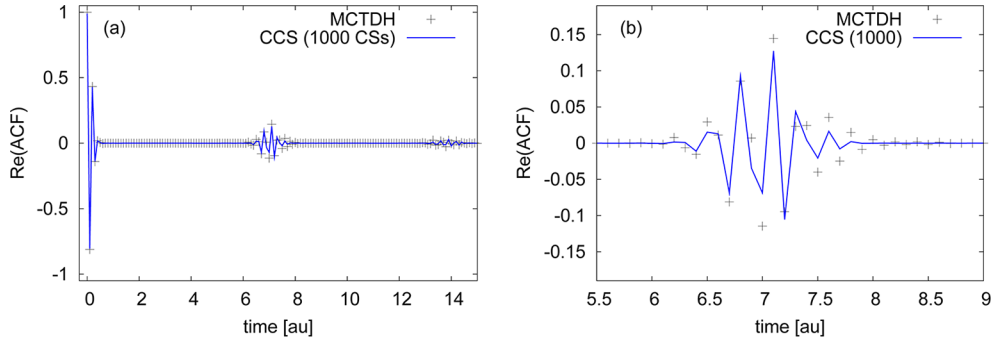

Figure 6. Real part of the autocorrelation function for the 10D HH problem with CCS with the basis of 1000 CSs (solid line) compared with results from MCTDH (crosses) (frame a) and the first recurrence (frame b).

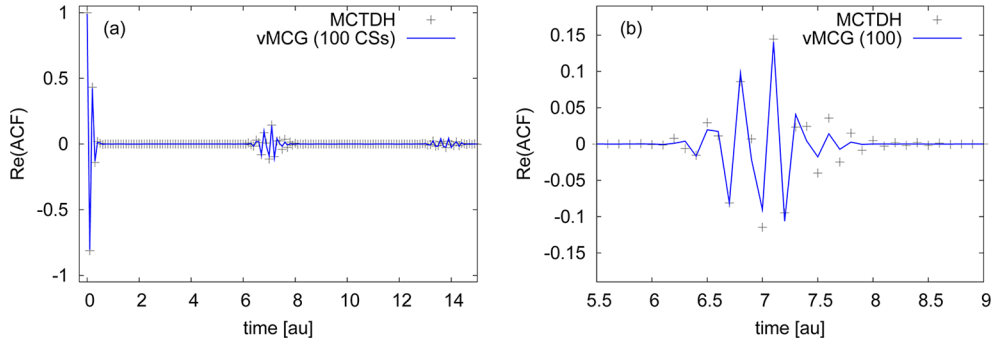

Figure 7. Real part of the autocorrelation function for the 10D HH problem with vMCG with the basis of 100 CSs (solid line) compared with results from MCTDH (crosses) (frame a) and the first recurrence (frame b).

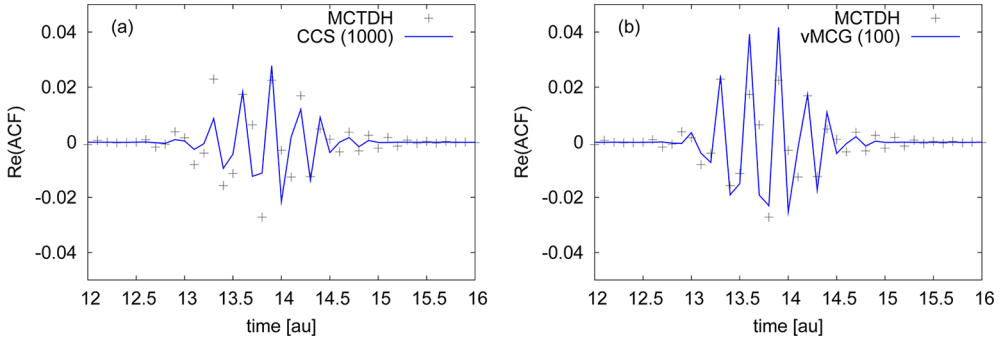

Figure 8. Comparison of the second recurrence of the autocorrelation function for the 10D HH problem obtained with CCS (1000 CSs) and vMCG (100 CSs) (frame a and b). Results from MCTDH are shown by crosses.

Table 1. Deviation of the CCS Result from That of MCTDH for a Different Number of Initial Basis-Vectors

number of initial basis-vectors	deviation from MCTDH first recurrence	deviation from MCTDH second recurrence	running time [sec]	compression [n = 0.9905]	remaining basis-vectors	number of variational parameters (number of remaining parameters are in brackets)
25	0.9495	0.2857	1.7	4.16	10	25 (10)
500	0.3752	0.2213	730.5	1.73	195	500 (195)
1000	0.3062	0.1519	2965.8	1.55	425	1000 (425)

Table 2. Comparison of the vMCG Result with That of MCTDH for a Different Number of Initial Basis-Vectors

number of initial basis-vectors	deviation from MCTDH first recurrence	deviation from MCTDH second recurrence	running time [sec]	compression [n = 0.9905]	remaining basis-vectors	number of variational parameters (number of remaining parameters are in brackets)
10	1.0586	0.2419	0.4	7.055	1	111 (11)
50	0.5252	0.2650	24.7	3.24	20	550 (220)
100	0.2536	0.1639	138.7	2.65	35	1100 (385)

dx.doi.org/10.1021/jp310976d | J. Phys. Chem. A 2013, 117, 6948−6959

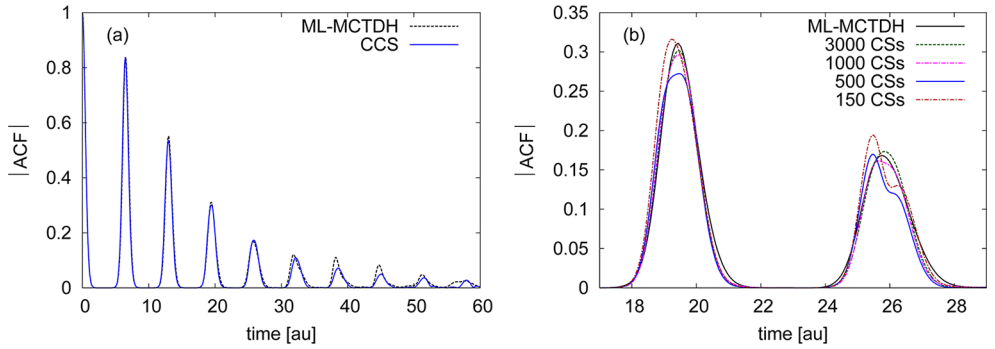

Figure 9. Absolute value of the autocorrelation function for the 18D HH problem with CCS (3000CSs) and its convergence (frame a and b). Results from ML-MCTDH are shown by a dashed line in frame a.

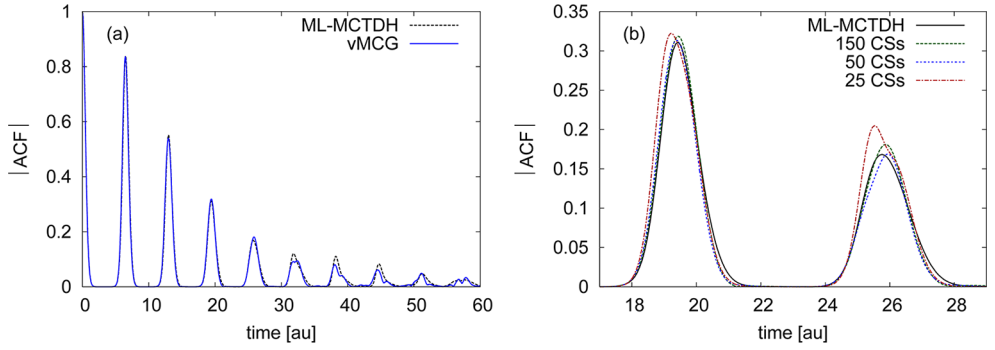

Figure 10. Absolute value of the autocorrelation function for the 18D HH problem with vMCG (150CSs) and its convergence (frame a and b). Results from ML-MCTDH are shown by dashed line in frame a.

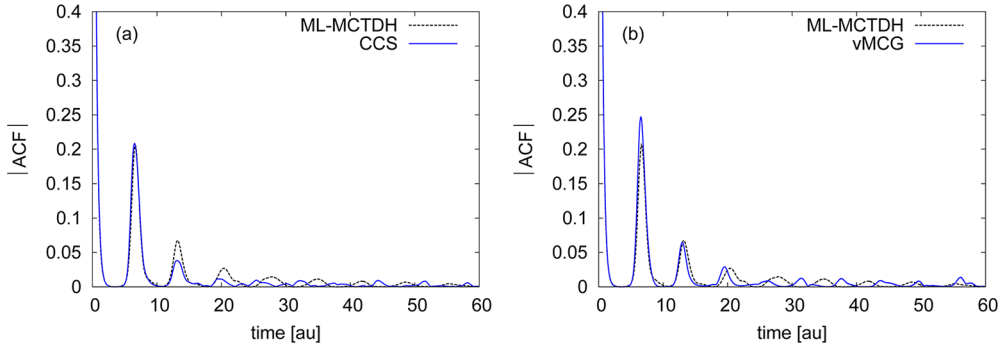

Figure 11. Absolute value of the autocorrelation function for the 18D HH problem of strong coupling, with CCS (4000 CSs) (frame a) and with vMCG (200 CSs) (frame b). Results from ML-MCTDH are shown by dashed line in both frames.

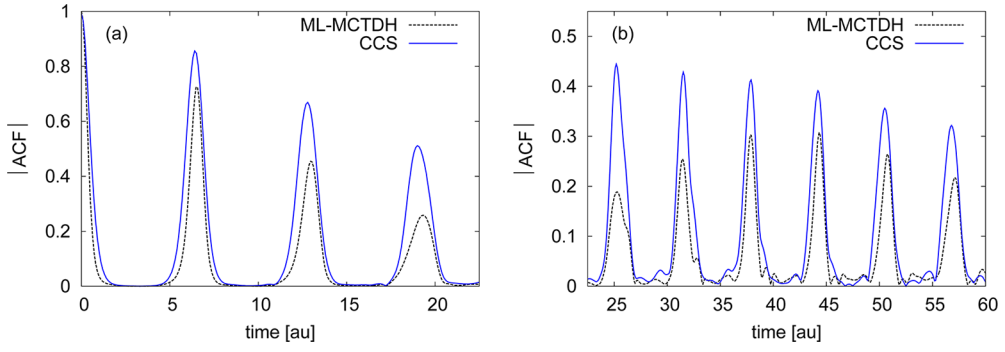

Figure 12. Absolute value of the autocorrelation function for the 1458D HH problem (System 1) with CCS (500CSs) (frames a and b). Results from ML-MCTDH are shown by dashed lines in both frames.

dx.doi.org/10.1021/jp310976d | J. Phys. Chem. A 2013, 117, 6948−6959

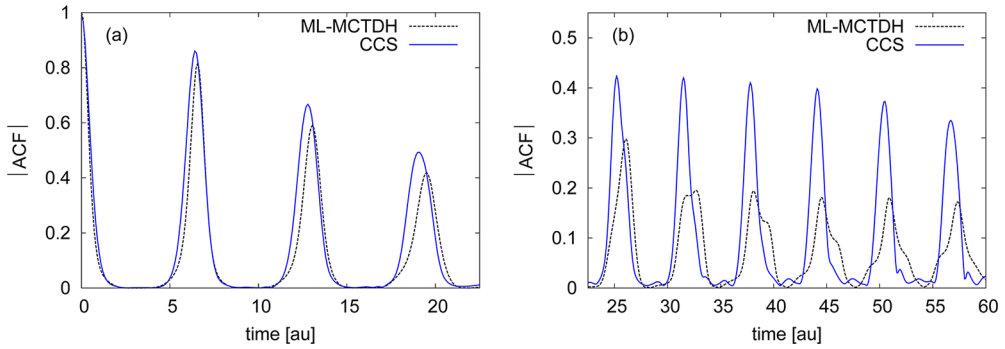

Figure 13. Absolute value of the autocorrelation function for the 1458D HH problem (System 2) with CCS (500CSs) (frames a and b). Results from ML-MCTDH are shown by dashed lines in both frames. The difference between CCS and the ML-MCTDH autocorrelation function for System 2 is less than the difference between the ML-MCTDH results for System 1 and System 2.

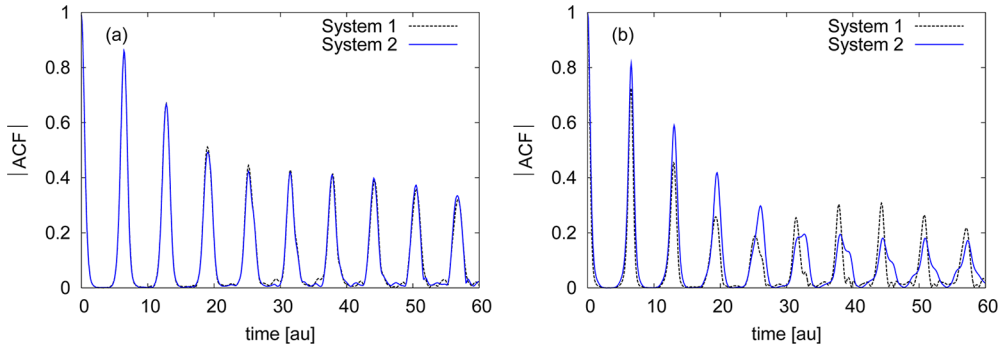

Figure 14. Comparison of absolute value of the autocorrelation function for the 1458D HH problem. The CCS autocorrelation functions for System 1 and System 2 shown in frame a coincide. The ML-MCTDH results for the two systems are shown at frame b.

this work. As can be seen from Figure 11, even a basis set that becomes very small provides a reasonably accurate result for the autocorrelation function.

Since benchmark results were available for the 1458D HH model,[23] we endeavored to attempt similar calculation with vMCG and CCS methods. In ref 23, two cases of the 1458D HH model were investigated. In the first case, called System 1, only the modes 486 and 487 were initially excited to $|\Psi^{(486)}(0)\rangle = |\Psi^{(487)}(0)\rangle = |q = 2, p = 0\rangle$. In the second case, called System 2, only the modes 729 and 730 were stretched as $|\Psi^{(729)}(0)\rangle = |\Psi^{(730)}(0)\rangle = |q = 2, p = 0\rangle$. In both systems, the excited modes are in the middle of the chain of coupled oscillators, far from its ends. Thus, the expectation is that the results from the two exact propagations should lie very close to one another. The difference between the two cases is that for System 1 the mode combination in ML-MCTDH is not good. Quoting ref 23, System 1 "represents an example of the wrong choice of tree structure" in ML-MCTDH. On the contrary, the mode combination and ML-MCTDH tree structure for System 2 correctly accounts the coupling of system modes. Simulations of the 1458D HH model would be very time-consuming for vMCG albeit not impossible. Even a basis set as small as 5 Gaussian coherent sets would include 1458 × 5+5 = 7295 variational parameters, which would require the solution of a system of 7295 linear equations (eqs 1.3) for derivatives of the parameters. On the other hand, CCS was able to tackle this very high-dimensional problem, yielding the results shown in Figures 12−14 for the basis of 500 CSs sampled with Sampling S3. Figure 12 shows that CCS autocorrelation function deviates from that of ML-MCTDH for System 1 very quickly, but for System 2 the agreement is much better. Figure 13 indicates that for System 2 the first two recurrences are in good agreement with ML-MCTDH. Unlike ML-MCTDH, results from CCS for System 1 and System 2 are identical as shown in Figure 14. CCS deviates from ML-MCTDH at later time.

We know from previous experience with CCS and related techniques, that at longer times the quality of CCS basis always deteriorates because (a) the CSs run away from each other and eventually stop exchanging amplitudes, and (b) CCS trajectories may guide basis in the wrong place. As a result, at longer times, CCS works as a semiclassical technique. Good sampling of the basis set is crucial for the efficiency and convergence of CCS, and the same can be said about vMCG or any other trajectory-based method. MCTDH is also a short time method, and it provides accurate results only if appropriate mode combination is found.

V. CONCLUSIONS

In this paper the numerical implementation of the modified vMCG equations was discussed. The results are directly compared with those obtained by CCS on equal formal footing. The tests and comparisons have been made for 1D harmonic, 1D Morse oscillator, and for 2D, 6D, 10D and 18D HH models. For the same basis set size, vMCG is more accurate, but for the same number of variational parameters, the quality of vMCG and CCS propagations is similar. Convergence and efficiency of CCS has been investigated previously, and the modified vMCG method shows very similar numerical behavior in terms of convergence of results and norm-conservation. The main result of this paper is that for the test systems considered here, our implementation of the modified version of vMCG equations works without regulariz-

dx.doi.org/10.1021/jp310976d | J. Phys. Chem. A 2013, 117, 6948−6959

ing and inverting the matrix **D** in eq 1.3, which significantly reduces computational costs. We also show once again that multidimensional quantum systems are within the reach of the trajectory based methods.

It is interesting to discuss the future of various trajectory-based methods for quantum molecular dynamics simulations where "on the fly" ab initio dynamics is the current trend. Many ab initio techniques such as multiple spawning (AIMS),[9,30] multiconfigurational Ehrenfest dynamics (MCE),[31] which is a generalization of CCS, and "on the fly" implementation of vMCG exist.[32,33] In such methods, the potential energy surfaces are calculated by applying an electronic structure package along the trajectory, which is the most expensive part of calculations. Having fewer vMCG trajectories may therefore have an advantage over the methods which use predetermined trajectories. On the other hand, methods like CCS/MCE allow running the trajectories one by one independently from each other which is not possible in vMCG, where trajectories are coupled with each other. Independent trajectories allow a detailed exploration of the dynamically relevant part of the PES prior to actual quantum dynamics calculation. Many electronic structure points can be accumulated and fit with the modern algorithms.[1,2] Perhaps a combination of vMCG and techniques that use predetermined trajectories will provide an optimum solution in the future.

APPENDIX

A1. Working Equations of Modified vMCG

Derivation of the equations of motion for $|\Psi(a,\mathbf{z})\rangle$ from the time-dependent variational principle enables us to investigate CCS and vMCG on the same formal footing. The Euler–Lagrange eqs 2.16 for dynamic parameters $a_i(t)$ and $\mathbf{z}_i(t)$ can be obtained separately from the Lagrangian (eq 2.15) as

$$\frac{\partial\Lambda}{\partial a} - \frac{\mathrm{d}}{\mathrm{d}t}\frac{\partial\Lambda}{\partial \dot{a}^*} = 0 \quad \text{and} \quad \frac{\partial\Lambda}{\partial \mathbf{z}} - \frac{\mathrm{d}}{\mathrm{d}t}\frac{\partial\Lambda}{\partial \dot{\mathbf{z}}^*} = 0 \tag{A1.1}$$

Performing the variation for amplitudes $a_i^*(t)$ gives

$$i\sum_j \mathbf{\Omega}_{ij}\dot{a}_j - \sum_j \mathbf{\Omega}_{ij}a_j\mathbf{H}_{\mathrm{ord}}(\mathbf{z}_i^*, \mathbf{z}_j) + i\sum_j \mathbf{\Omega}_{ij}a_j\left((\mathbf{z}_i^* - \mathbf{z}_j^*)\dot{\mathbf{z}}_j + \frac{\mathbf{z}_j^*\dot{\mathbf{z}}_j}{2} - \frac{\dot{\mathbf{z}}_j^*\mathbf{z}_j}{2}\right) = 0 \tag{A1.2}$$

and the variation of $\mathbf{z}_i^*(t)$ is

$$i\sum_j \mathbf{\Omega}_{ij}a_i^*\dot{a}_j(\mathbf{z}_j - \mathbf{z}_i) - \sum_j \mathbf{\Omega}_{ij}a_i^*a_j\left(i\dot{\mathbf{z}}_j - \frac{\partial\mathbf{H}_{\mathrm{ord}}(\mathbf{z}_i^*, \mathbf{z}_j)}{\partial\mathbf{z}_i^*}\right) + i\sum_j \mathbf{\Omega}_{ij}a_i^*a_j(\mathbf{z}_j - \mathbf{z}_i)^T\left((\mathbf{z}_i^* - \mathbf{z}_j^*)\dot{\mathbf{z}}_j + \frac{\mathbf{z}_j^*\dot{\mathbf{z}}_j}{2} - \frac{\dot{\mathbf{z}}_j^*\mathbf{z}_j}{2} + i\mathbf{H}_{\mathrm{ord}}(\mathbf{z}_i^*, \mathbf{z}_j)\right) = 0 \tag{A1.3}$$

For the sake of greater stability and better robustness, it is convenient to introduce a smoothing preexponential factor to describe the rapidly oscillating amplitudes a_j:

$$a_j = d_j \exp(iS_j) \tag{A1.4}$$

where S can be calculated from the classical action:

$$S_j = \int_{t_1}^{t_2}\left[\frac{i}{2}(\mathbf{z}_j^*\dot{\mathbf{z}}_j - \dot{\mathbf{z}}_j^*\mathbf{z}_j) - \mathbf{H}_{\mathrm{ord}}(\mathbf{z}_j^*, \mathbf{z}_j)\right]\mathrm{d}t \tag{A1.5}$$

With this preexponential factor, eq A1.2 can be rewritten as

$$\sum_j \mathbf{\Omega}_{ij}\exp(iS_j)\dot{d}_j + \sum_j \mathbf{\Omega}_{ij}\exp(iS_j)d_j(\mathbf{z}_j^* - \mathbf{z}_i^*)\dot{\mathbf{z}}_j = -i\sum_j \mathbf{\Omega}_{ij}\exp(iS_j)d_j(\mathbf{H}_{\mathrm{ord}}(\mathbf{z}_i^*, \mathbf{z}_j) - \mathbf{H}_{\mathrm{ord}}(\mathbf{z}_j^*, \mathbf{z}_j)) \tag{A1.6}$$

and eq A1.3 becomes

$$\sum_j \mathbf{\Omega}_{ij}\exp(i(S_j - S_i))d_i^*(\mathbf{z}_j - \mathbf{z}_i)\dot{d}_j + \sum_j \mathbf{\Omega}_{ij}\exp(i(S_j - S_i))d_i^*d_j[1 + (\mathbf{z}_j - \mathbf{z}_i)(\mathbf{z}_j^* - \mathbf{z}_i^*)]\dot{\mathbf{z}}_j = -i\sum_j \mathbf{\Omega}_{ij}\exp(i(S_j - S_i))d_i^*d_j\left[(\mathbf{H}_{\mathrm{ord}}(\mathbf{z}_i^*, \mathbf{z}_j) - \mathbf{H}_{\mathrm{ord}}(\mathbf{z}_j^*, \mathbf{z}_j))(\mathbf{z}_j - \mathbf{z}_i) + \frac{\partial\mathbf{H}_{\mathrm{ord}}(\mathbf{z}_i^*, \mathbf{z}_j)}{\partial\mathbf{z}_i^*}\right] \tag{A1.7}$$

The time evolution of $|\Psi(t)\rangle$ can be described by solving the equations for $d_i(t)$, $S_i(t)$, and $\mathbf{z}_i(t)$. In the case of CCS, the equations of motion for $\mathbf{z}_i(t)$ are given by Hamilton's equations:

$$\dot{\mathbf{z}}_j = -i\frac{\partial\mathbf{H}_{\mathrm{ord}}(\mathbf{z}_j^*, \mathbf{z}_j)}{\partial\mathbf{z}_j^*} \tag{A1.8}$$

This can be obtained from eq A1.6 if all terms containing small overlaps $\mathbf{\Omega}_{ij}$ between different CSs are neglected. In CCS, the equations for the amplitudes (preexponential factors) are still the same as eq A1.6. Although the trajectories (eq A1.8) are not fully variational, the CCS technique is still fully quantum because it relies on the exact coupled equations for the amplitudes. It has been shown in CCS that better stability is achieved by smoothing the amplitude by eq A1.4. In vMCG, both fully variational eqs A1.5 and A1.6 are used, and these are in principle equivalent to those of original vMCG theory.[15] The equations are forming a system of linear equations for the dynamical variables $d_i(t)$ and $\mathbf{z}_i(t)$:

$$\sum_j \sum_{(n)} D_{ij}^{(1+m,1+n)}\dot{\alpha}_j^{(1+n)} = b_i^{(1+m)} \tag{A1.9}$$

where

$$\dot{\alpha}_j^{(1+n)} = [\dot{d}_j, \dot{z}_j^{(1)}, ..., \dot{z}_j^{(n)}] \tag{A1.10}$$

This set of linear equation can be written in matrix form as

$$\begin{bmatrix} D1_{ij} & D2_{ij}^{(1)} & \dots & D2_{ij}^{(n)} \\ D3_{ij}^{(1)} & D4_{ij}^{(1,1)} & \dots & D4_{ij}^{(1,n)} \\ \vdots & \vdots & \ddots & \vdots \\ D3_{ij}^{(m)} & D4_{ij}^{(m,1)} & \dots & D4_{ij}^{(m,n)} \end{bmatrix}\begin{bmatrix} \dot{d}_j \\ \dot{z}_j^{(1)} \\ \vdots \\ \dot{z}_j^{(n)} \end{bmatrix} = \begin{bmatrix} b1_i \\ b2_i^{(1)} \\ \vdots \\ b2_i^{(m)} \end{bmatrix} \tag{A1.11}$$

dx.doi.org/10.1021/jp310976d | J. Phys. Chem. A 2013, 117, 6948–6959

where in this block matrix every letter represents an $N \times N$ matrix with the following elements:

$$
\begin{aligned}
D1_{ij} &= \mathbf{\Omega}_{ij} \exp(iS_j) \\
D2_{ij}^{(n)} &= \mathbf{\Omega}_{ij} \exp(iS_j) d_j (z_i^{*(n)} - z_j^{*(n)}) \\
D3_{ij}^{(m)} &= \mathbf{\Omega}_{ij} \exp(i(S_j - S_j)) d_i^* (z_j^{(m)} - z_i^{(m)}) \\
D4_{ij}^{(m,n)} &= \mathbf{\Omega}_{ij} \exp(i(S_j - S_j)) d_i^* d_j [\delta_{(mn)} + (z_j^{(m)} - z_i^{(m)}) \\
&\quad (z_i^{*(n)} - z_j^{*(n)})] \\
b1_i &= -i \sum_j \mathbf{\Omega}_{ij} \exp(iS_j) d_j (\mathbf{H}_{\mathrm{ord}}(\mathbf{z}_i^*, \mathbf{z}_j) \\
&\quad - \mathbf{H}_{\mathrm{ord}}(\mathbf{z}_j^*, \mathbf{z}_j)) \\
b2_i^{(n)} &= -i \sum_j \mathbf{\Omega}_{ij} \exp(i(S_j - S_j)) d_i^* d_j \Bigg[(z_j^{(m)} - z_i^{(m)}) \\
&\quad (\mathbf{H}_{\mathrm{ord}}(\mathbf{z}_i^*, \mathbf{z}_j) - \mathbf{H}_{\mathrm{ord}}(\mathbf{z}_j^*, \mathbf{z}_j)) \\
&\quad + \frac{\partial \mathbf{H}_{\mathrm{ord}}(\mathbf{z}_i^*, \mathbf{z}_j)}{\partial z_i^{*(n)}} \Bigg]
\end{aligned}
\tag{A1.12}
$$

The only improvement is that they are written for the smooth preexponential factor d rather than for the amplitude itself. Although an attempt has been made in the original vMCG[15] to take the oscillating part away from the amplitude, the exact way of how this should be done can be important. In the current formulation, the smoothening is done in a fashion similar to the CCS technique, and the matrix $\mathbf{D}$ appears to be small, smooth and sparse and reasonably well behaved.

Numerically, CCS can be implemented easier than vMCG. The two differences in the program code are the way $\dot{d}$ and $\dot{z}$ are calculated and the derivative matrix of the Hamiltonian. The structure of the working matrix of CCS is simpler as it contains coefficients for $\dot{d}$ only, thus it is independent of the dimension of the system. The other significant difference is that CCS uses only the diagonal elements of the derivative of the Hamiltonian, whereas for vMCG all the elements for all dimensions have to be calculated. However, implementation and coding of a method has to be done only once, and, once implemented, the complicated vMCG algorithm can be very useful. A new problem requires only programming of the new Hamiltonian and its derivative.

A2. Numerical Instabilities of Sampling S2

Let us set one of the initial CSs to $|\Psi(0)\rangle = |\mathbf{z}_o\rangle$ such as in eq 3.5

$$
|\mathbf{z}_{j=1}\rangle = |\mathbf{z}_o\rangle \tag{A2.1}
$$

Then the initial amplitude is

$$
C_i = \langle \mathbf{z}_i | \mathbf{z}_0 \rangle = \begin{bmatrix} 1 \\ C_2 \\ \vdots \\ C_i \end{bmatrix} \tag{A2.2}
$$

and the overlap-matrix will be

$$
\mathbf{\Omega}_{ij} = \langle \mathbf{z}_i | \mathbf{z}_j \rangle = \begin{bmatrix} 1 & C_2 & \dots & C_j \\ C_2^* & 1 & \dots & \langle \mathbf{z}_2 | \mathbf{z}_j \rangle \\ \vdots & \vdots & \ddots & \vdots \\ C_j^* & \langle \mathbf{z}_i | \mathbf{z}_2 \rangle & \dots & 1 \end{bmatrix} \tag{A2.3}
$$

Amplitude d is calculated from the set of linear equations

$$
C_j = \sum_j \mathbf{\Omega}_{ij} d_i \tag{A2.4}
$$

and the only solution for A2.4 with matrix A2.3 and vector A2.2 is

$$
d_i^* = \begin{bmatrix} 1 \\ 0 \\ \vdots \\ 0 \end{bmatrix} \quad \text{and} \quad d_j = [1, 0, ..., 0] \tag{A2.5}
$$

The initial action $S_j = 0$ and therefore $\exp(iS_j) = 1$. With these conditions the components of matrix $\mathbf{D}$ and vector $\mathbf{b}$ in eqs A1.11 will be as follows:

$$
\begin{aligned}
D1_{ij} &= \mathbf{\Omega}_{ij} \\
D2_{ij}^{(n)} &= \mathbf{\Omega}_{ij} (z_i^{*(n)} - z_j^{*(n)}) \text{ if } i > 2,\ j = 1 \text{ and } 0 \\
&\quad \text{elsewhere} \\
D3_{ij}^{(n)} &= \mathbf{\Omega}_{ij} (z_j^{(m)} - z_i^{(m)}) \text{ if } i = 2,\ j > 1 \text{ and } 0 \\
&\quad \text{elsewhere} \\
D4_{ij}^{(m,n)} &= \delta_{(mn)} \text{ if } i = j = 1 \text{ and } 0 \text{ elsewhere} \\
b1_i &= -i \sum_j \mathbf{\Omega}_{ij} (\mathbf{H}_{\mathrm{ord}}(\mathbf{z}_i^*, \mathbf{z}_j) - \mathbf{H}_{\mathrm{ord}}(\mathbf{z}_j^*, \mathbf{z}_j)) \\
&\quad \text{if } i > 2,\ j = 1 \text{ and } 0 \text{ elsewhere} \\
b2_i^{(n)} &= -i \sum_j \frac{\partial \mathbf{H}_{\mathrm{ord}}(\mathbf{z}_i^*, \mathbf{z}_j)}{\partial z_i^{*(n)}} \text{ if } i = j = 1 \text{ and } 0 \\
&\quad \text{elsewhere}
\end{aligned}
\tag{A2.6}
$$

It can be seen that in matrix $\mathbf{D}$, every $(n+i)(i+1)$th column and every $(m+j)(j+1)$th row contains zeros only. This makes $\mathbf{D}$ singular, although the matrix is not inverted; therefore the problem with det $\mathbf{D} = 0$ is still solvable. The under-determined system of linear equations in the case of vMCG will lead to numerical difficulties, which requires regularization. In the case of CCS, only $D1$ and $b1$ are calculated; this system has unambiguous solutions.

The probability that in a Monte Carlo sampled basis (used for sampling S1 and S3) one basis vector will be equivalent to the initial wave function is practically zero. However, if a sampling condition similar to S2 is required, vMCG can always be regularized at the very first step by either regularizing matrix $\mathbf{D}$ or by propagating the first few steps with CCS, which is a simpler and physically more justifiable solution.

AUTHOR INFORMATION

Corresponding Author

*E-mail: cmmr@leeds.ac.uk; d.shalashilin@leeds.ac.uk.

Notes

The authors declare no competing financial interest.

■ ACKNOWLEDGMENTS

This work has been supported by EPSRC grants EP/I014500/1 and EP/J001481/1. We thank Irene Burghardt and Graham Worth for useful discussions, Mathias Nest for providing the MCTDH benchmark data, Hans-Dieter Meyer for providing the ML-MCTDH results and Christopher Symonds for useful editorial comments.

■ REFERENCES

(1) Bowman, J. M.; Braams, B. J.; Carter, S.; Chen, C.; Czako, G.; Fu, B.; Huang, X.; Kamarchik, E.; Sharma, A. R.; Shepler, B. C.; Wang, Y.; Xie, Z. Ab-Initio-Based Potential Energy Surfaces for Complex Molecules and Molecular Complexes. *J. Phys. Chem. Lett.* **2010**, *1* (12), 1866−1874.

(2) Bowman, J. M.; Czako, G.; Fu, B. High-Dimensional Ab Initio Potential Energy Surfaces for Reaction Dynamics Calculations. *Phys. Chem. Chem. Phys.* **2011**, *13* (18), 8094−8111.

(3) Bowman, J. M.; Carter, S.; Huang, X. MULTIMODE: A Code to Calculate Rovibrational Energies of Polyatomic Molecules. *Int. Rev. Phys. Chem.* **2003**, *22* (3), 533−549.

(4) Bowman, J. M.; Carrington, T.; Meyer, H.-D. Variational Quantum Approaches for Computing Vibrational Energies of Polyatomic Molecules. *Mol. Phys.* **2008**, *106* (16−18), 2145−2182.

(5) Heller, E. J. Frozen Gaussians - A Very Simple Semi-Classical Approximation. *J. Chem. Phys.* **1981**, *75* (6), 2923−2931.

(6) Herman, M. F.; Kluk, E. A Semiclassical Justification for the Use of Non-spreading Wavepackets in Dynamics Calculations. *Chem. Phys.* **1984**, *91* (1), 27−34.

(7) Child, M. S.; Shalashilin, D. V. Locally Coupled Coherent States and Herman−Kluk Dynamics. *J. Chem. Phys.* **2003**, *118* (5), 2061−2071.

(8) Kay, K. G. Semiclassical Initial Value Treatments of Atoms and Molecules. *Annu. Rev. Phys. Chem.* **2005**, *56*, 255−280.

(9) Ben-Nun, M.; Martinez, T. J. Ab Initio Quantum Molecular Dynamics. *Adv. Chem. Phys.* **2002**, *121*, 439−512.

(10) Burghardt, I.; Meyer, H. D.; Cederbaum, L. S. Approaches to the Approximate Treatment of Complex Molecular Systems by the Multiconfiguration Time-Dependent Hartree Method. *J. Chem. Phys.* **1999**, *111* (7), 2927−2939.

(11) Shalashilin, D. V.; Child, M. S. Basis Set Sampling in the Method of Coupled Coherent States: Coherent State Swarms, Trains, and Pancakes. *J. Chem. Phys.* **2008**, *128* (5), 054102−054102.

(12) Shalashilin, D. V.; Child, M. S. The Phase Space CCS Approach to Quantum and Semiclassical Molecular Dynamics for High-Dimensional Systems. *Chem. Phys.* **2004**, *304* (1−2), 103−120.

(13) Shalashilin, D. V.; Child, M. S. Multidimensional Quantum Propagation with the Help of Coupled Coherent States. *J. Chem. Phys.* **2001**, *115* (12), 5367−5375.

(14) Sawada, S. I.; Heather, R.; Jackson, B.; Metiu, H. A Strategy for Time-Dependent Quantum-Mechanical Calculations Using a Gaussian Wave Packet Representation of the Wave-Function. *J. Chem. Phys.* **1985**, *83* (6), 3009−3027.

(15) Worth, G. A.; Burghardt, I. Full Quantum Mechanical Molecular Dynamics Using Gaussian Wavepackets. *Chem. Phys. Lett.* **2003**, *368* (3−4), 502−508.

(16) Kramer, P.; Saraceno, M. *Geometry of the Time-Dependent Variational Principle in Quantum Mechanics*; Springer: NewYork, 1981.

(17) Shalashilin, D. V.; Burghardt, I. Gaussian-Based Techniques for Quantum Propagation from the Time-Dependent Variational Principle: Formulation in Terms of Trajectories of Coupled Classical and Quantum Variables. *J. Chem. Phys.* **2008**, *129* (8), 084104.

(18) Frenkel, J. *Wave Mechanics, Advanced General Theory*; Clarendon Press: Oxford, 1934.

(19) Broeckhove, J.; Lathouwers, L.; Kesteloot, E.; Vanleuven, P. On the Equivalence of Time-Dependent Variational Principles. *Chem. Phys. Lett.* **1988**, *149* (5−6), 547−550.

(20) Kay, K. G. The Matrix Singularity Problem in the Time-Dependent Variational Method. *Chem. Phys.* **1989**, *137* (1−3), 165−175.

(21) McLachlan, A. D. Variational Solution of Time-Dependent Schrodinger Equation. *Mol. Phys.* **1964**, *8* (1), 39.

(22) Nest, M.; Meyer, H. D. Benchmark Calculations on High-Dimensional Henon−Heiles Potentials with the Multi-Configuration Time Dependent Hartree (MCTDH) Method. *J. Chem. Phys.* **2002**, *117* (23), 10499−10505.

(23) Vendrell, O.; Meyer, H. D. Multilayer Multiconfiguration Time-Dependent Hartree Method: Implementation and Applications to a Henon−Heiles Hamiltonian and to Pyrazine. *J. Chem. Phys.* **2011**, *134* (4), 044135.

(24) Meyer, H.-D., Gatti, F., Worth, G. A. *Multidimensional Quantum Dynamics. MCTDH Theory and Applications*; Wiley-VCH: Weinheim, Germany, 2007.

(25) Sherratt, P. A. J.; Shalashillin, D. V.; Child, M. S. Description of Multidimensional Tunnelling with the Help of Coupled Coherent States Guided by Classical Hamiltonians with Quantum Corrections. *Chem. Phys.* **2006**, *322* (1−2), 127−134.

(26) Shalashilin, D. V.; Child, M. S. Time Dependent Quantum Propagation in Phase Space. *J. Chem. Phys.* **2000**, *113* (22), 10028−10036.

(27) Shalashilin, D. V.; Jackson, B. Guiding Paths and Time-Dependent Basis Sets for Wavefunction Propagation. *Chem. Phys. Lett.* **2000**, *318* (4−5), 305−313.

(28) Sklarz, T.; Kay, K. G. Semiclassical Initial Value Treatment of Correlation Functions. *J. Chem. Phys.* **2004**, *120* (6), 2606−2617.

(29) Brewer, M. L. On the Scaling of Semiclassical Initial Value Methods. *J. Chem. Phys.* **1999**, *111* (14), 6168−6170.

(30) Levine, B. G.; Coe, J. D.; Virshup, A. M.; Martinez, T. J. Implementation of Ab Initio Multiple Spawning in the MOLPRO Quantum Chemistry Package. *Chem. Phys.* **2008**, *347* (1−3), 3−16.

(31) Saita, K.; Shalashilin, D. V. On-the-Fly Ab Initio Molecular Dynamics with Multiconfigurational Ehrenfest Method. *J. Chem Phys.* **2012**, *137* (22), 22A506−8.

(32) Worth, G. A.; Robb, M. A.; Lasorne, B. Solving the Time-Dependent Schrodinger Equation for Nuclear Motion in One Step: Direct Dynamics of Non-adiabatic Systems. *Mol. Phys.* **2008**, *106* (16−18), 2077−2091.

(33) Lasorne, B.; Worth, G. A.; Robb, M. A. Excited-State Dynamics. *Wiley Interdiscip. Rev.: Comput. Mol. Sci.* **2011**, *1* (3), 460−475.